ACS APPLIED MATERIALS & INTERFACES

Research Article

www.acsami.org

Mechanosensitive Liposomes as Artificial Chaperones for Shear-Driven Acceleration of Enzyme-Catalyzed Reaction

Tomotaka Natsume and Makoto Yoshimoto*

Department of Applied Molecular Bioscience, Yamaguchi University, 2-16-1 Tokiwadai, Ube, 755-8611, Japan

Supporting Information

ABSTRACT: Mechanosensitive liposomes were prepared and applied to continuously accelerate the glucose oxidase (GO) reaction in shear flow. The liposome membrane was composed of a ternary lipid mixture containing 20 mol % negatively charged lipid and 30 mol % cholesterol. The liposomes encapsulating GO and catalase were passed through microtubes with inner diameter of 190 or 380 μm at 25 °C to induce the catalytic oxidation of 10 mM glucose with simultaneous decomposition of H_2O_2 produced. The liposomal GO showed significantly low reactivity in the static liquid system because of the permeation resistance of lipid membranes to glucose. On the other hand, the enzyme activity of liposomal GO observed at the average shear rate of 7.8×10^3 s^{-1} was significantly larger than its intrinsic activity free of mass transfer effect in the static liquid system. The structure of liposomes was highly shear-sensitive as elucidated on the basis of shear rate-dependent physical stability of liposomes and membrane permeability to 5(6)-carboxyfluorescein as well as to GO. Thus, the above shear-driven acceleration of GO reaction was indicated to be caused by the free GO molecules released from the structurally altered liposomes at high shear rates. Moreover, the shear-induced denaturation of free GO was completely depressed by the interaction with the sheared liposomes with the chaperone-like function. The shear-sensitive liposomal GO system can be a unique catalyst that continuously accelerates and also decelerates the oxidation reaction depending on the applied shear rate.

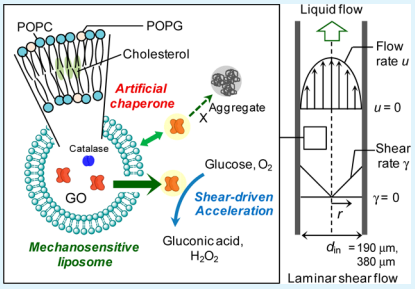

KEYWORDS: *mechanosensitive liposomes, glucose oxidase, shear rate, artificial chaperone, accelerated enzyme reaction*

1. INTRODUCTION

Hydrodynamic shear force induces structural and functional responses of cells.[1] It is well documented that vascular endothelial cells perceive the shear stress generated by blood flow and transduce it into intracellular functions.[2] In such cellular mechanotransduction events, lipid bilayer membranes may play a crucial role because of their structural flexibility[3] and direct contacting with flowing fluids. Shear force also affects the molecular level of structure of biopolymers such as DNA[4] and proteins.[5−7] Shear-induced biologically relevant phenomena have received much attention because of their potential applications.[8,9] Holme et al.[10] reported the shear stress-induced permeabilization of liposomes composed of amidophospholipids.[11] This is applicable to the mechanical stress-triggered drug delivery where drugs are released from liposomes in response to intense shear stress at a plaque of blood vessels. Because shear stress is generated by any flowing fluid at various scales, shear-induced structures and functions of biomolecules, lipid membranes, and cells would be utilized for the design and operation of bioreactors.[1]

Microfluidics can offer highly controllable fluid systems which are applicable to various analytical, separation, and reaction processes.[12−15] Quite interestingly, some enzyme-catalyzed reactions are accelerated by the laminar flow in microfluidics,[16−18] which would be useful in the analytical and synthetic chemistry. On the other hand, the enzyme molecules undergo conformational change and deactivation through being successively exposed to shear stress.[19−22] Although the mechanism for shear-induced acceleration of enzyme reaction is not fully understood, the above observations show that the shear flow can provide quite different environment for the enzyme activity compared to the static liquid system even under the physiological pH and temperatures.

In the cellular system, folding intermediates of proteins and heat-induced conformationally changed proteins are facilitated to become native forms by the actions of molecular chaperones.[23] Chaperone proteins can effectively interact with hydrophobic sites of aggregate-prone proteins. On the other hand, shear stress causes conformational changes of proteins leading to exposure of their hydrophobic domains to the liquid phase.[20] Thus, it is implied that the stability of proteins in shear flow increases in the presence of materials with the chaperone-like function. For example, α-crystalline can inhibit fluid flowing-induced formation of amyloid fibrils of conformationally changed proteins.[24] Molecular chaperones or chaperone-like proteins are not the best materials to be applied to shear flow especially at high shear rates because of their potential deactivation and high cost. In this context, artificial chaperones with sufficient mechanical stability may be candidates for stabilizing the enzyme activity in shear flow. So far, materials

Received: December 26, 2013
Accepted: February 19, 2014
Published: February 19, 2014

such as nanogel,[25] soft nanotube hydrogels,[26] and functional polymers[27] were reported to function as artificial chaperones in refolding or thermal denaturation processes of proteins. However, to the best of our knowledge, little is studied on the artificial chaperone that can function in shear flow. Liposomes, which also function as artificial chaperones in the refolding of chemically unfolded proteins,[28,29] would be attractive to be utilized in shear flow because of their controllable size, physical stability, and shear-sensitivity.[30,31]

In this work, we propose a novel liposomal system for accelerating an enzyme reaction in shear flow. This system utilizes the mechanosensitivity of lipid membrane that enables to release the liposome-encapsulated enzymes into the shear field. Effect of liposome membranes on the stability of enzyme activity was clarified to evaluate the chaperone-like function of liposomes in shear flow. Laminar shear flow was generated at relatively high average shear rates ($\sim 7.8 \times 10^3$ s^{-1}) using the liquid flow through microtubes with inner diameter of 190 and 380 μm. The model enzyme reaction employed was the glucose oxidase-catalyzed oxidation of glucose with simultaneous decomposition of H_2O_2 produced.[32,33] The controlled GO-catalyzed reaction in flowing fluids would be useful for the selective sensing of glucose[34] and the production of gluconic acid.[35]

2. EXPERIMENTAL SECTION

2.1. Materials. 1-Palmitoyl-2-oleoyl-*sn*-glycero-3-phosphocholine (POPC) and 1-palmitoyl-2-oleoyl-*sn*-glycero-3-phosphoglycerol (POPG) were obtained from NOF (Tokyo, Japan). POPC is zwitterionic, whereas POPG is negatively charged. Glucose oxidase from *Aspergillus niger* (GO; EC 1.1.3.4, $M_r \approx 180\,000$)[36] was obtained from Toyobo (Osaka, Japan). Cholesterol, β-D-glucose, 3,3-dimethoxybenzidine dihydrochloride (*o*-dianisidine), sodium cholate, horseradish peroxidase (HRP) and catalase from *bovine liver* (EC 1.11.1.6, $M_r \approx 240\,000$) were obtained from Wako Pure Chemical Industries (Osaka, Japan). 5(6)-Carboxyfluorescein (CF) was from Sigma-Aldrich (St. Louis, MO, USA). Bovine serum albumin (BSA, IgG-free and protease-free) was from Jackson ImmunoResearch Laboratories (West Grove, PA, USA). All chemicals were used as received. Water used was deionized and sterilized using an instrument Elix 3UV (Millipore, Billerica, MA, USA). The minimum resistance to the water was 15 MΩ cm.

2.2. Preparation of Liposomes Encapsulating GO and Catalase, and Liposomes Encapsulating CF. A ternary lipid mixture (POPC:POPG:cholesterol = 50:20:30 in molar ratio) was dissolved in 4.0 mL of chloroform and the solvent was removed by using a rotary evaporator. This procedure was further performed twice using diethylether instead of chloroform. The residual organic solvent molecules were removed under the reduced pressure in the dark with a freeze-dryer. The thin lipid film formed was hydrated with 2.0 mL of a 50 mM Tris-HCl/100 mM NaCl buffer solution (pH 7.4) containing 5.0 g/L GO and 5.0 g/L catalase. The mixture of multilamellar vesicles and enzymes was frozen in a refrigerant (dry ice/ethanol) for 7 min and thawed in a water bath at 37 °C for 7 min (7 cycles) to enhance the transformation of small vesicles into larger ones. The vesicles suspension thus obtained was passed through a polycarbonate membrane with mean pore diameter of 200 nm using an extrusion device Liposofast from Avestin (Ottawa, Canada).[37] Nonencapsulated enzyme molecules were removed from the enzymes-containing liposomes by using gel permeation chromatography (GPC) with a sepharose 4B column (1.0 (id) × 20 cm). "Empty" liposomes were also prepared with the same procedure as above except that the dry lipid film was hydrated with an enzyme-free Tris buffer solution. The CF-containing liposomes (denoted as CFLs) were prepared with the method reported previously.[30] In this case, CFLs were passed through 100 or 200 nm membrane pores for sizing. The concentration of POPC was measured using a phosphatidylcholine quantification kit from Wako Pure Chemical Industries.[38]

2.3. Measurement of Enzyme Activity of GO. The enzyme activity of GO was measured at 25 °C in the Tris buffer solution with 10 mM glucose as substrate. The GO reaction gives gluconic acid and H_2O_2 from glucose and molecular oxygen. The initial rate of H_2O_2 produced was determined based on the HRP-catalyzed oxidation of *o*-dianisidine with H_2O_2. The initial concentrations of HRP and *o*-dianisidine in the reaction mixture (1.5 mL) were 0.2 g/L and 0.33 mM, respectively. An increase in the concentration of oxidized *o*-dianisidine was continuously followed based on the absorbance at 460 nm (ε_{460} = 11 300 $M^{-1}cm^{-1}$)[39] in a quartz cuvette with 1.0 cm optical path length using a spectrophotometer (V-630BIO, Jasco, Tokyo, Japan). We confirmed that the catalase activity contained in the liposomal system did not interfere with the above activity measurements. Intrinsic GO activity in the liposomal system was measured in the presence of 40 mM sodium cholate for complete solubilization of liposome membranes.[40]

2.4. Measurement of Enzyme Activity of Catalase. The enzyme activity of catalase was measured at 25 °C with 10 mM H_2O_2 as substrate.[41] The time course of H_2O_2 decomposition was followed in the cuvette based on the absorbance at 240 nm (ε_{240} = 39.4 M^{-1} cm^{-1})[42] with the spectrophotometer. Intrinsic activity of catalase in the liposomal system was determined in the presence of 40 mM sodium cholate.

2.5. Measurements of Mean Size and Size Distribution. Size distribution of liposomes was measured by the dynamic light scattering method with an ELSZ-2plus instrument (Otsuka Electronics, Osaka, Japan) equipped with a semiconductor laser as a light source. The wavelength and an angle of the light were 660 nm and 160°, respectively. The size distribution was calculated with the Marquardt algorithm. Mean diameter (D_P) of liposomes was determined with the Einstein-Stokes relation using a refractive index of 1.33. Polydispersity index (PI) of liposomes was determined based on the size distribution. The Tris buffer solution used for diluting liposome suspensions was filtrated through a membrane (Milex PVDF, Millipore, Billerica, MA) with pore diameter of 0.22 μm. All measurements were performed at 25 °C in triplicate.

2.6. Oxidation of Glucose in a Reactor with External Liquid Circulation through Microtubes. Figure 1 shows the schematic drawing of a reaction system used which consists of a quartz cuvette and four parallel tygon tubes with the length L of 0.40 m and the inner diameter d_{in} of 190 or 380 μm. The simultaneous liquid flow through the microtubes was generated using a peristaltic pump instrument ECOLINE VC-MS/CA4-12 (ISMATEC, Glattbrugg, Switzerland).

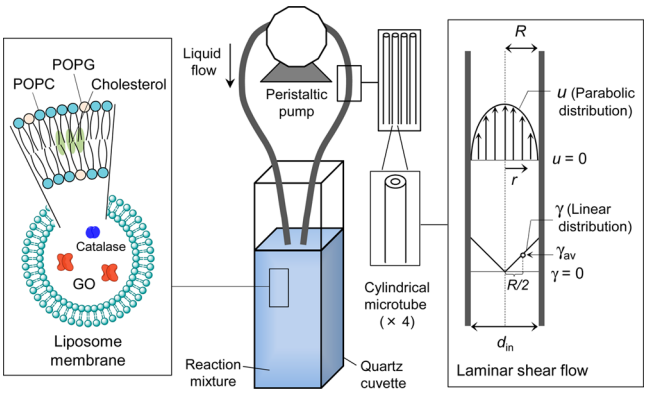

Figure 1. Schematic drawing of a reactor consists of a quartz cuvette suspending liposomes encapsulating GO and catalase with external liquid circulation through four parallel microtubes (d_{in} = 190 or 380 μm). Dimension of the cuvette was 1.0 cm × 1.0 cm × 4.5 cm in height. The length of each microtube was 0.40 m. The cuvette was bathed in a water bath thermostatted at 25 °C. The distribution of liquid flow rate u and shear rate γ within the microtube is also shown.

The maximum average flow rate u_{av} was 0.37 and 0.30 m/s at d_{in} of 190 and 380 μm, respectively. The Reynolds number Re is a dimensionless number that can be a measure of the flow regime in a cylindrical tube flow path. Re is defined as $Re = d_{in}u_{av}\rho/\mu$, where ρ is the fluid density, and μ is the viscosity of the fluid (μ = 0.94 mPa s). The Re value can be calculated as $Re \leq 75$. This means the laminar flow regime in each microtube. Since the liposome suspension was a Newtonian fluid, a parabolic velocity distribution of liquid flow u should be formed in the mictrotubes as $u = \{\Delta PR^2/(4\mu L)\}\{1 - (r/R)^2\}$, where r is the distance from the center of a microtube, R is the radius of the microtube ($R = d_{in}/2$), and ΔP is the pressure difference between inlet and outlet of the microtube ($\Delta P = 8\mu L u_{av}/R^2$).[43] As a measure of the shear condition in the microtubes, we employed average shear rate γ_{av}. The shear rate γ at any r is described as $\gamma = du/dr = \Delta Pr/2\mu L$. Thus, a linear shear rate distribution should be formed in the microtubes, giving the γ_{av} value as $\gamma_{av} = \Delta PR/(4\mu L)$ at $r = R/2$. Accordingly, the average shear stress τ_{av} can be calculated as $\tau_{av} = \gamma_{av}\mu$. The present operation condition gives the γ_{av} values of 7.9×10^2 to 7.8×10^3 s^{-1}. The maximum shear rate ($\gamma_{max} = 2\gamma_{av}$) is generated at the wall of microtubes.

To initiate the catalytic oxidation of glucose, the Tris buffer solution suspending the liposomes encapsulating GO and catalase was charged into the cuvette and a glucose solution was added to give the concentrations of total lipid and glucose of 1.0 mM and 10 mM, respectively. The liquid circulation was then immediately started. The volume (V_M) of liquid phase within the microtubes relative to the total volume ($V_T \leq 2.0$ mL) of a reaction mixture ($V_M/V_T \approx 0.1$) was identical regardless of the value of d_{in}. Aliquots were periodically withdrawn from the cuvette to quantify the residual concentration of glucose with a kit from Wako Pure Chemical Industries. The concentration of H_2O_2 was also measured based on the HRP-catalyzed reaction as reported previously.[44] The oxidation reaction was also performed with 3.3×10^{-2} g/L free GO and 5.0×10^{-2} g/L free catalase in the presence ([lipid] = 1.0 mM) and absence of empty liposomes. To evaluate the effect of adsorption of enzymes to the inner surface of microtubes on the reaction, the reaction operation was partly performed using the microtubes which were pretreated with a 1.0 g/L BSA solution. This treatment was performed at relatively low shear rate $\gamma_{av} = 7.9 \times 10^2$ s^{-1} for 30 min followed by rinsing twice with the Tris buffer solution at the same flow condition. The activity of GO and catalase in the liposomal system was measured before and after the reaction operation. The activity measurements were performed with and without 40 mM sodium cholate. To evaluate the interaction of liposome membranes with the inner surface of microtubes, the empty liposomes ([lipid] = 1.0 mM) were continuously passed through the microtubes and the concentration of lipid in the cuvette was followed.

2.7. Measurements of Stability of Liposomal and Free Enzymes in Shear Flow. The liposomes encapsulating GO and catalase were sheared by passing through the microtubes at the total lipid concentration of 1.0 mM in the absence of glucose using the apparatus shown in Figure 1. Then, the intrinsic enzyme activity of GO and catalase in the cuvette was followed. For measuring the stability of free enzymes, the above measurement was performed with respect to the Tris buffer solution containing 1.0×10^{-2} g/L free GO or 7.6×10^{-2} g/L free catalase. The stability of free GO was also measured at the same enzyme concentration as above in the presence of empty liposomes ([lipid] = 1.0 mM).

2.8. Determination of Leakage of GO from Liposomes. The free GO molecules, which might be released from liposome interior under shear stress condition, were separated from liposome-encapsulated enzymes by using the GPC. The liposomes encapsulating GO and catalase were sheared at $\gamma_{av} = 3.1 \times 10^3$ s^{-1} by passing through the microtubes for 180 min at the total lipid concentration of 5.0 mM and then, the liposome suspension was loaded on a sepharose 4B column. The collected fractions were analyzed based on the lipid concentration and the intrinsic GO activity which was converted to the enzyme concentration. The fractional amount of GO leaked was calculated as the amount of GO in the later eluting peak relative to the total amount of GO eluted.[40]

2.9. Measurement and Analysis of CF-Release from Liposomes Suspended in Shear Flow. The CFLs were sheared at 25 °C using the microtube flow system (Figure 1). Aliquots were withdrawn from the cuvette at any operation time t for measuring the fluorescence intensity I_t of CF at 25 °C with a spectrofluorometer instrument FP-770 from Jasco (Tokyo, Japan). The excitation and emission wavelengths for the measurement were 490 and 517 nm, respectively. The fluorescence intensity I_∞ at the permeation equilibrium was determined in the presence of 40 mM sodium cholate. Then, the fractional release R_{CF} of CF from liposomes was calculated as $R_{CF} = (I_t - I_0)/(I_\infty - I_0)$, where I_0 represents the initial CF fluorescence intensity. The operation time t was converted to the effective shearing time t_{eff} as $t_{eff} = t\,(V_M/V_T)$ to compare the kinetics of CF-release in the present shearing system with that in the previously reported system.[31] On the basis of the mass balance with respect to CF,[30,45] the permeability coefficient P_{CF} was determined as $P_{CF} = ka^{-1}$, where a is the specific surface area of CFL ($a = 6/D_P$) and k is the slope of straight line obtained by plotting $-\ln(1 - R_{CF})$ vs. t_{eff}.

3. RESULTS AND DISCUSSION

3.1. Characteristics of Liposomal GO-Catalyzed Reaction in Shear Flow. The liposomes encapsulating GO and catalase were monodisperse (polydispersity index PI = 0.062 ± 0.024) and had the mean diameter D_P of 149 ± 2 nm. The average number of GO and catalase molecules per liposome was estimated to be 12.8 ± 2.5 and 6.6 ± 0.4, respectively (see Table S1 in the Supporting Information). The liposomal GO-catalyzed oxidation of 10 mM glucose was performed at 25 °C in shear flow. The flow regime in microtubes partly deviates from the laminar flow because of peristaltic motion, potentially causing intense shear stress. The local change in the flow condition may have an influence on the structure of liposomes. However, we employed the average shear rate (γ_{av}) in the laminar flow region to represent the shear stress condition in the microtubes considering significantly short time for passing through the non-laminar flow region compared to the average residence time through a microtube. The reaction was also performed in a test tube ($\gamma = 0$). Figure 2A shows the fractional conversion of glucose as a function of operation time at various γ_{av} values. It should be noted that for all of the reactions, the H_2O_2 produced by the glucose oxidation was not detected throughout the operation period of 180 min because of sufficient catalytic action of the liposomal catalase. At $\gamma = 0$, the liposomal GO shows significantly low reactivity because of the strong permeation resistance of lipid membranes to the substrate molecules.[40,46,47] The reaction time course at $\gamma = 0$ is also shown for the micellar system which was obtained by solubilzing the liposomes with cholate to liberate the enzyme molecules (broken curve in Figure 2A). The micellar GO reaction exhibits larger oxidation rate than the liposomal one at $\gamma = 0$ because the former reaction proceeds under the reaction control with negligible mass transfer effect. The apparent oxidation rate of glucose ($-r_{G,app}$) catalyzed by the liposomal GO tends to increase as the γ_{av} value increases (Figure 2B). It is worth noting that the $-r_{G,app}$ values obtained at 3.1×10^3 $s^{-1} \leq \gamma_{av}$ are larger than the rate of micellar GO reaction. This result indicates the shear flow-driven acceleration of GO-catalyzed reaction. The above results demonstrate that the liposomal GO system can exhibit a wide range of apparent enzyme activity which is tunable on the basis of the applied shear rate.

3.2. Mechanosensitivity of Liposome Membranes. We evaluated high shear rates-induced structural change in liposomes composed of POPC, POPG and cholesterol based on the permeability of lipid membranes and the physical stability of liposomes. We selected the above mixed liposome

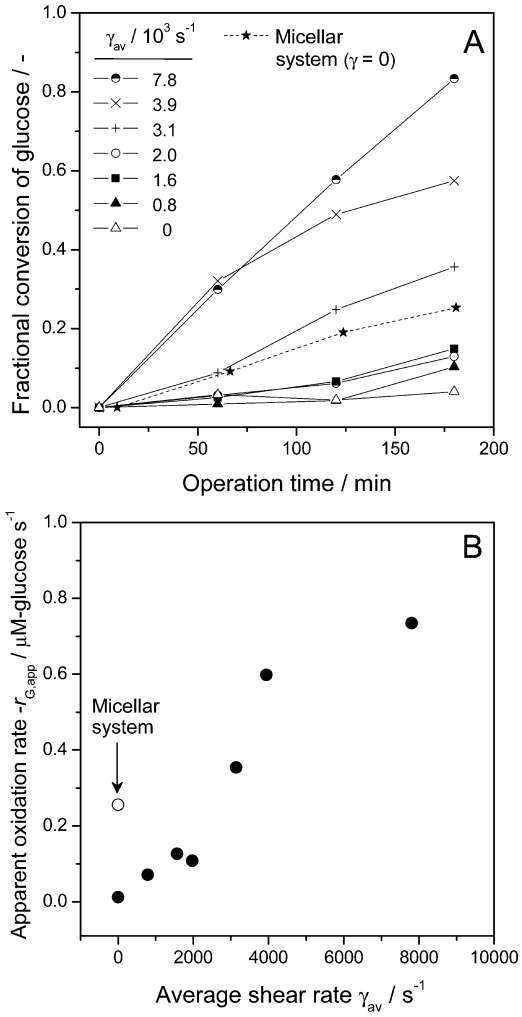

Figure 2. (A) Time courses of fractional conversion of 10 mM glucose catalyzed by liposomes encapsulating GO and catalase at various average shear rates γ_{av} at 25 °C. The total lipid concentration was 1.0 mM. The overall concentration of GO was 1.0 ×10^{-2} g/L. Broken curves and filled stars represent the data for the reaction catalyzed by micellar enzyme system at γ = 0. (B) Effect of γ_{av} on the apparent oxidation rate of glucose $-r_{G,app}$ catalyzed by liposomal GO. The rate for micellar enzyme-catalyzed reaction is also shown (empty circle).

because its membrane structure can be altered even at 25 °C at relatively low shear rates ($\gamma \leq 1.5 \times 10^3$ s^{-1}),[30] whereas the shear-dependent permeability of the membrane composed of POPC alone was reported only at a higher temperature.[31] Furthermore, negatively charged liposomes such as PG-containing ones can form clusters in the presence of cations,[48,49] which is quite useful for developing drug vehicles based on a novel strategy[48] and increasing shear-sensitivity of liposomes.[30] Membrane permeability of a hydrophilic compound can be a measure of the degree of membrane perturbation.[31,45,50] The 5(6)-carboxyfluorescein (CF)-containing liposome (CFL) with D_P of 150 nm was passed through the microtubes with d_{in} of 190 or 380 μm at 25 °C and the fractional CF released R_{CF} was followed. In a test tube (γ = 0), the lipid membrane is practically impermeable, giving R_{CF} < 0.01 at the incubation period of 180 min. Figures 3 depict the effects of effective shearing time t_{eff} and γ_{av} on the R_{CF} value. The rate of CF-release at d_{in} = 190 μm is seen to increase as the γ_{av} value increases (Figure 3A). This is also the case for the CFL sheared at d_{in} = 380 μm (Figure 3B). We also performed the experiments with respect to the CFL with D_P = 188 nm and obtained similar results to the above (Figure S1). The permeability coefficient P_{CF} of the CF molecules was calculated on the basis of the unsteady-state mass balance with respect to CF[30,45] and plotted as a function of γ_{av} (Figure 4). The data obtained for the CFL with D_P = 188 nm are also shown for comparison. The P_{CF} value clearly increases as the γ_{av} value increases regardless of the size of CFLs. It is also seen that the CFL with D_P of 188 nm shows larger P_{CF} values than the smaller CFL. Effect of shearing was examined at γ_{av} = 7.8 ×10^3 s^{-1} on the size distribution of CFLs with D_P = 150 nm (Figure 5A) and 188 nm (Figure 5B). These CFLs are not significantly affected in their size distribution by the applied shear stress. The above results reveal that local structural change in the hydrophobic core of liposome membranes is induced by the laminar shear flow, whereas overall vesicular structure is practically maintained. A closer look of Figure 5A indicates that the shearing causes a small decrease in the size of liposomes. We examined the possible interaction of liposome membranes with the inner surface of microtubes on the basis of the lipid concentration in the liquid phase (see Figure S2 in the Supporting Information). Practically no change in the lipid

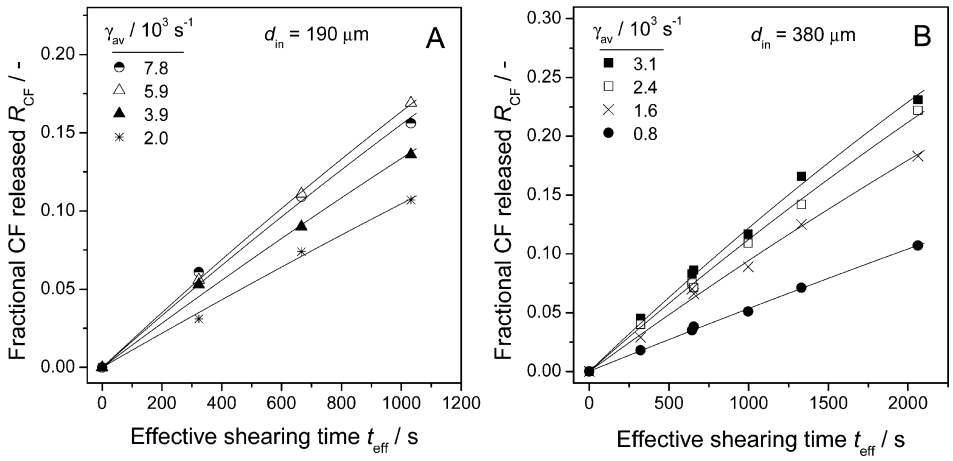

Figure 3. Time courses of fractional CF released R_{CF} from CFLs with D_P = 150 nm at various γ_{av} values at 25 °C. CFL suspension was sheared in the microtubes with d_{in} = 190 μm (A) and 380 μm (B). Solid curves represent the calculated time courses, $R_{CF} = \{1 - \exp(-P_{CF}at_{eff})\}$. The value of $P_{CF}a$ corresponds to the slope of straight line obtained by plotting $-(1 - R_{CF})$ vs. t_{eff}.

dx.doi.org/10.1021/am405992t | ACS Appl. Mater. Interfaces 2014, 6, 3671−3679

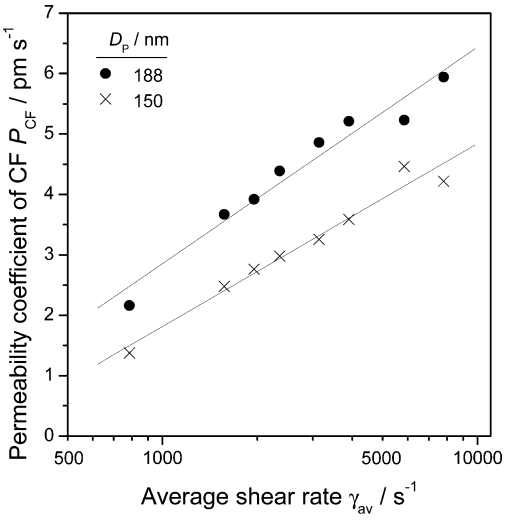

Figure 4. Effect of average shear rate γ_{av} on permeability coefficient P_{CF} of CF through liposome membranes.

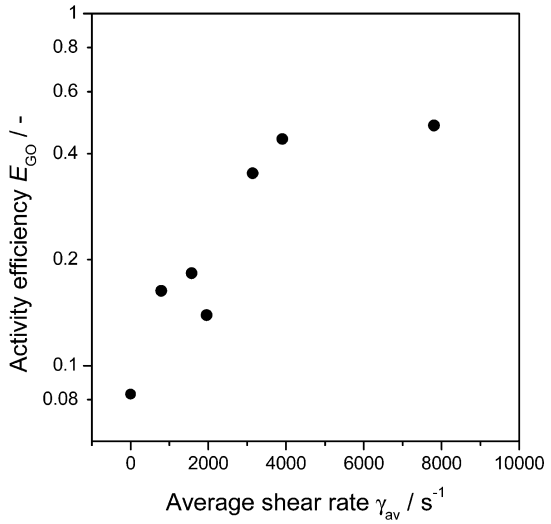

Figure 6. Effect of average shear rate γ_{av} on activity efficiency E_{GO} of liposome-encapsulated GO molecules. The E_{GO} value was determined at the operation time of 180 min at 25 °C.

concentration was observed for 180 min at $\gamma_{av} = 7.8 \times 10^3$ s^{-1}, demonstrating that the liposome-microtube interaction was negligible. The above results imply that the small extent of disruption of liposomes occurs through the hydrodynamic force derived from shear flow. The P_{CF} values obtained here for the POPC/POPG/cholesterol liposomes at 25 °C are larger than the values reported for the liposomes composed of POPC alone at 40 °C.[31] The high sensitivity of the present liposomes to shear stress may be derived from the structural heterogeneity of the cholesterol-containing membrane.

3.3. Leakage of GO Molecules from Liposomes. We measured leakage of the GO molecules from liposomes suspended in shear flow. The molecular mass of GO is about 480 times larger than that of CF. Activity efficiency E_{GO} was defined with respect to GO as $E_{GO} = A_{L,S}/A_{I,0}$, where $A_{L,S}$ is the activity of GO observed in the liposomal system at the shearing operation time of 180 min and $A_{I,0}$ is the intrinsic activity at the initial state. The $A_{I,0}$ value can be determined by solubilizing liposomes with cholate. Figure 6 shows the E_{GO} value as a function of γ_{av}. Significantly small E_{GO} value can be confirmed at $\gamma = 0$. The value tends to increase up to 0.48 as the γ_{av} value increases to 7.8×10^3 s^{-1}, reaching a plateau at 3.9×10^3 s$^{-1} \leq \gamma_{av}$. This result suggests that the GO molecules are released from liposome interior to the shear field. The GO-containing liposomes, which were sheared at $\gamma_{av} = 3.1 \times 10^3$ s^{-1} for 180 min, were loaded on a sepharose 4B column in order to separate free (leaked) GO from liposomes. Relatively small E_{GO} value of 0.15 was obtained in this case probably because the lipid concentration employed was 5 times higher than that used for the glucose oxidation reaction. Figure 7 shows the elution profile obtained based on the concentrations of lipid and GO. A single peak at the fraction no. 7 is seen with respect to the concentration of lipid, showing the elution of liposomes within the peak. On the other hand, two peaks were observed with respect to the concentration of GO at the fraction nos. 7 and 15. Considering the elution profile of lipid as well as the significant difference in the size between a liposome and a free GO molecule, the earlier eluting peak corresponds to the liposome-encapsulated GO molecules and the later peak corresponds to the leaked GO ones. We found that the present GPC separation causes little leakage of the liposomal GO molecules based on the following observation. In the preparation of enzyme-containing liposomes, we also used the column for separating free (non-encapsulated) enzymes as described in the section 2.2. The apparent activity of liposome-

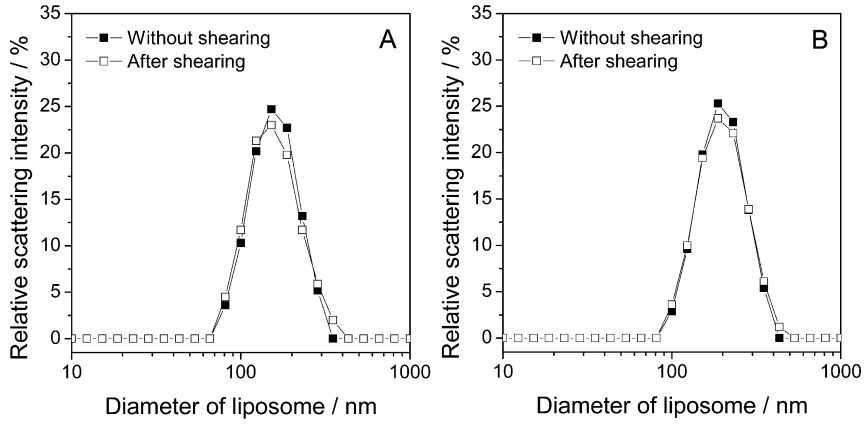

Figure 5. Effect of shearing on size distribution of CFLs with initial D_P of (A) 150 and (B) 188 nm. Shearing was performed at $\gamma_{av} = 7.8 \times 10^3$ s^{-1} at 25 °C for $t_{eff} = 1.0 \times 10^3$ s.

dx.doi.org/10.1021/am405992t | ACS Appl. Mater. Interfaces 2014, 6, 3671−3679

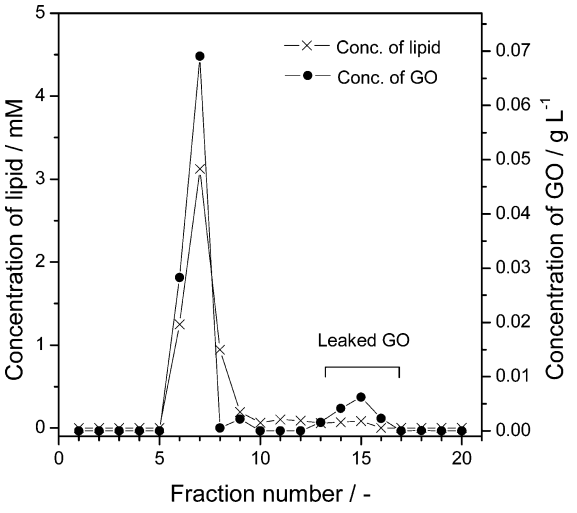

Figure 7. GPC profiles of liposomes encapsulating GO and catalase sheared at γ_{av} = 3.1 × 10^3 s^{-1} for 180 min at 25 °C at the total lipid concentration of 5.0 mM. The peak around fraction 7 corresponds to liposome-encapsulated GO and the peak around fraction 15 corresponds to free (leaked) GO.

encapsulated GO recovered from the column was on average 3.8 ± 0.6 % (mean ± standard deviation, n = 6) of its intrinsic activity. The low apparent activity showed that the lipid membrane exhibited large permeation resistance to glucose and also the liposome suspension contained negligible amount of free GO molecules. The above results clearly demonstrate that the sepharose 4B column cannot promote leakage of the liposome-encapsulated GO molecules. Therefore, the free GO molecules detected in Figure 7 correspond to the molecules which are released from liposomes not during the GPC but in the shear flow. The amount of GO leaked relative to the total amount of GO eluted was determined as 0.16. This value agrees very closely with the above E_{GO} value of 0.15, indicating that the E_{GO} value corresponds to the fractional amount of GO molecules leaked by the shearing. We measured the size distribution of enzyme-containing liposomes with and without shearing at γ_{av} = 7.8 × 10^3 s^{-1} for 180 min (see Figure S3 in the Supporting Information). The shearing treatment causes no significant change in the distribution, although a slight decrease in the size of liposomes is seen. The mean diameter of liposomes was 183 ± 1 nm at the initial state and 177 ± 2 nm after the shearing. The above results favor the major mechanism where the liposomal GO molecules pass through lipid membranes with a little effect on the overall vesicular structure of liposomes. Shear stress-triggered partial disruption of liposomes is also suggested, which can be an alternative minor mechanism of the release of liposomal GO. The γ_{av} value of 7.8 × 10^3 s^{-1} corresponds to the average shear stress τ_{av} of 7.3 Pa. At the wall of microtubes, intense shear stress of 14.6 Pa is generated, which would cause significant release of the macromolecular GO from liposomes.

3.4. Chaperone-Like Function of Liposomes toward Enzyme Molecules in Shear Flow. The above results show that release of the GO molecules from liposomes is induced in a shear rate-dependent manner. The free GO molecules potentially undergo structural change in shear flow. The GO-containing liposomes were passed through microtubes at γ_{av} = 7.8 × 10^3 s^{-1} and the GO activity was followed. The E_{GO} value of 0.31 was obtained in this case at the operation time of 360 min. This indicates that 31% of the liposome-encapsulated GO molecules were released into the shear field. The result obtained is shown in Figure 8. In the figure, no loss of the GO

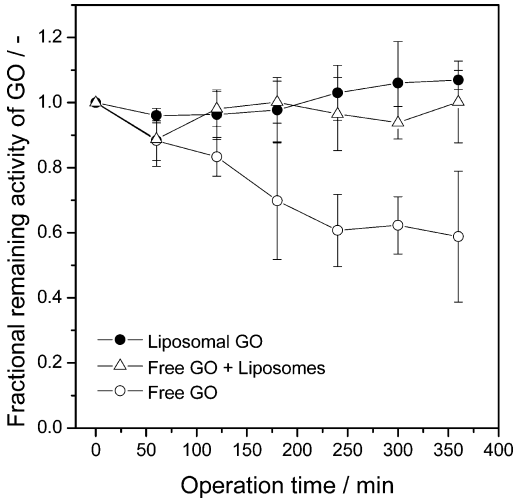

Figure 8. Time courses of fractional remaining activity of liposomal GO (filled circles), free GO plus empty liposomes ([lipid] = 1.0 mM) (empty triangles) and free GO alone (empty circles) at γ_{av} = 7.8 × 10^3 s^{-1} at 25 °C. The concentration of free GO was fixed at 1.0 × 10^{-2} g/L. Data represent mean ± standard deviation.

activity is seen at 360 min. This result demonstrates that the released GO molecules undergo little change in their activity under the shear stress condition. In Figure 8, stability of the free GO activity in the shear flow is also shown for comparison. A progressive deactivation of free GO is seen during the shearing in the absence of liposome, exhibiting remaining activity of 59% at 360 min. Because practically no deactivation was seen in the static liquid system, the deactivation of free GO was regarded to be caused by the applied shear stress. We further examined the stability of free GO in the presence of empty liposomes at the same enzyme concentration as that employed for the free enzyme alone. Liposomes clearly stabilize the GO activity in the shear flow. Therefore, the liposome membrane can exhibit the chaperone-like function toward the free GO molecules. We found that the structure of free catalase was more sensitive to the shear flow compared to that of free GO probably because of fragility of the tetrameric catalase.[41] The enzyme activity of liposomal catalase was more stable than that of the free catalase under the shear stress condition (see Figure S4 in the Supporting Information). Liposome membranes consist of hydrophobic core and hydrophilic region exposed to the liquid phase. Hydrophobic patches are formed at the membrane-water interface of liposomes because of local fluctuation of the membranes, as previously elucidated based on the binding of a hydrophobic probe to POPC liposomes.[28] The surface of liposomes is, therefore, hydrophilic overall but considerably abundant in local hydrophobic sites. As observed in section 3.2, the extent of membrane perturbation and the partial disruption of liposomes are clearly dependent on the shear rate. These structural changes in liposome membranes can cause the formation of local hydrophobic sites on the surface of liposomes which can be the binding sites to the conformationally changed enzyme molecules.[28] On the other hand, conformational change of proteins is caused by hydrodynamic shear forces, as well documented for bovine serum albumin

(BSA)[6] and von Willebrand factor.[5] Shear stress also causes deactivation of enzymes.[19] Bekard et al.[6] reported that intramolecular hydrogen bonding and interactions between secondary structures of BSA were destabilized by the drag due to shear flow ($\gamma < 500\ s^{-1}$). These previous reports indicate that shear stress can induce the formation of conformationally changed GO and catalase molecules which may be prone to form inactive aggregates. Our results indicate that the conformationally changed enzyme molecules are stabilized through the hydrophobic interaction with structurally destabilized liposomes as artificial chaperones. Such mechanism would be similar to that proposed for the chaperone-like function of liposomes toward the refolding intermediates of several enzymes.[28,29]

3.5. Plausible Mechanism for Liposomal Enzyme-Catalyzed Reaction in Shear Flow. On the basis of the above results, we assume that the free GO molecules, which are released from liposomes by the shear stress, are responsible for the shear-driven accelerated oxidation of glucose catalyzed by the liposomal GO system. To verify this mechanism, we performed the free GO-catalyzed reaction in the presence of empty liposomes and free catalase at $\gamma = 0$ and at $\gamma_{av} = 7.8 \times 10^3\ s^{-1}$. The reaction was also performed with free GO at $\gamma = 0$ in the absence of liposomes. The results obtained are shown in Figure 9. At $\gamma = 0$, the oxidation reaction with liposomes gives

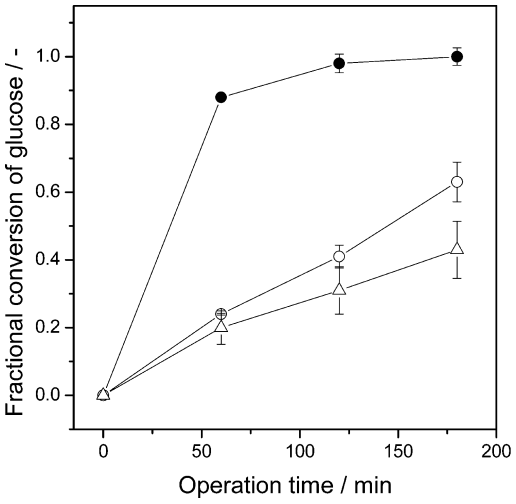

Figure 9. Time courses of fractional conversion of 10 mM glucose at 25 °C catalyzed by free GO with empty liposomes at $\gamma_{av} = 7.8 \times 10^3\ s^{-1}$ (filled circles) and at $\gamma = 0$ (empty circles). The time course is also shown for the oxidation of 10 mM glucose at 25 °C catalyzed by free GO at $\gamma = 0$ in the absence of liposomes (empty triangles). Concentrations of free GO and free catalase were 3.3×10^{-2} g/L and 5.0×10^{-2} g/L, respectively. Data represent mean ± standard deviation.

slightly larger rate than that without liposomes. Clearly, the reaction in the shear flow ($\gamma = 7.8 \times 10^3\ s^{-1}$) gives a significantly larger oxidation rate than the reactions in the static liquid system. This means that the free GO reaction can be accelerated by the shear flow in the presence of liposomes. To estimate the extent of shear-driven acceleration of the liposomal GO reaction, we calculated the reaction rate $-r'_G$ [mmol-glucose/(s g-GO)] based on the effective amount of GO as $-r'_G = -r_{G,app}/(E_{GO}C_{GO})$, where C_{GO} is the intrinsic concentration of GO in the reaction mixture. Figure 10 shows the effect of γ_{av} on $-r'_G$, which was calculated from the

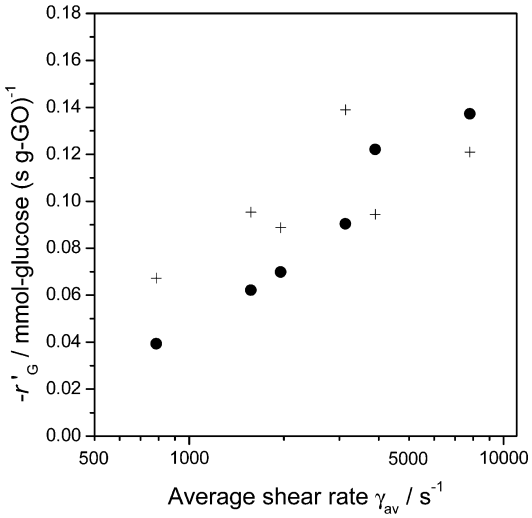

Figure 10. Effect of γ_{av} on the oxidation rate of glucose $-r'_G$ based on the effective amount of GO. Crosses represent the $-r'_G$ values obtained with the microtubes treated with a BSA solution prior to each reaction operation.

$-r_{G,app}$ values shown in Figure 2B. A plot of $-r'_G$ vs. log γ_{av} gives an approximately linear relationship (filled circles in Figure 10). Since the microtubes used offer significantly large surface-to-volume ratio, adsorption of the enzyme molecules to the solid surface needs to be clarified. We performed the glucose oxidation reaction using the microtubes treated with a BSA solution. The $-r'_G$ values obtained are plotted as a function of γ_{av} (crosses in Figure 10). Although the data show some scatter, the relationship between the two parameters is similar to that obtained without the BSA treatment. Therefore, the enzyme adsorption appears to have rather minor effect on the liposomal GO-catalyzed reaction in shear flow.

Recently, Wang et al.[18] reported that the free GO activity was enhanced in the laminar flow generated in a nanofluidic reactor compared to the activity in bulk solution. Similar phenomena were also reported for other enzyme-catalyzed reactions.[16,17,51] Tanaka et al.[16] reported that the horse radish peroxidase-catalyzed reaction was accelerated in a microchannel. Miyazaki et al.[51] reported that the hydrolytic activity of trypsin was enhanced by using a microchannel reactor. They pointed out the possible effect of the laminar flow-induced localization of enzyme molecules within the channel on acceleration of the enzyme reaction. It was also reported that the trypsin-substrate affinity increased in the shear flow based on the kinetic analysis.[52] In the present work, the laminar flow in microtubes can provide unique hydrodynamic properties including fluid mixing and the flow rate distribution giving the maximum rate of 0.37 m/s at the center of microtubes, which would affect the efficiency of liposomal GO-catalyzed reaction in the shear flow. Furthermore, one of the possible reasons for the shear-driven acceleration of GO-catalyzed reaction is the formation of an activated form of GO in the presence of liposomes in shear flow. The intermolecular interaction among the conformationally changed GO molecules is depressed because of the liposome-enzyme interaction. Subtle structural change of an enzyme molecule may influence its affinity toward glucose. The liposomal interface can continuously stabilize the reactive form of GO in the shear flow, although this needs to be further studied.

dx.doi.org/10.1021/am405992t | ACS Appl. Mater. Interfaces 2014, 6, 3671−3679

4. CONCLUSIONS

We succeeded in accelerating the GO reaction in a controlled manner using the mechanosensitive liposomes encapsulating GO and catalase. The shear-induced structural perturbation and partial disruption of lipid membranes composed of POPC, POPG and cholesterol (50:20:30 in molar ratio) triggered the release of the GO molecules into the shear field. The oxidation of glucose catalyzed by the released GO molecules was significantly accelerated in the presence of liposomes at the relatively high average shear rate of 7.8×10^3 s^{-1}. Moreover, liposome membranes stabilized the GO activity in the shear flow where the free enzyme molecules were readily deactivated in the absence of liposomes. In the static liquid, in clear contrast, the liposomal GO showed low reactivity because of the permeation resistance to glucose through the lipid membranes. The liposomal GO system can therefore exhibit a wide range of enzyme activity in response to the applied shear stress, which may find applications in blood flow-responsive drug vehicles and controlled oxidation reactions in microfluidics.

■ ASSOCIATED CONTENT

Supporting Information

Procedures for estimation of the liposomal contents of enzymes, the kinetics of CF-release from the CFL with D_p = 188 nm, the evaluation of liposome-microtube interaction, the size distribution of enzyme-containing liposomes with and without shearing, and the stability of liposomal and free catalase in shear flow. This material is available free of charge via the Internet at http://pubs.acs.org/.

■ AUTHOR INFORMATION

Corresponding Author

*E-mail: yosimoto@yamaguchi-u.ac.jp. Tel.: 81 836 85 9271. Fax: 81 836 85 9201.

Notes

The authors declare no competing financial interest.

■ ACKNOWLEDGMENTS

This work was supported in part by the Grant-in-Aid for Scientific Research (C) (no.25420833) from the Japan Society for the Promotion of Science (JSPS).

■ REFERENCES

(1) Chisti, Y. In *Encyclopedia of Industrial Biotechnology, Bioprocess, Bioseparation, and Cell Technology*; Flickinger, M. C., Ed.; Wiley: New York, 2010; Vol. 7, pp 4360−4398.

(2) Ando, J.; Yamamoto, K. Flow Detection and Calcium Signalling in Vascular Endothelial Cells. *Cardiovascular Res.* **2013**, *99*, 260−268.

(3) Gudi, S.; Nolan, J. P.; Frangos, J. A. Modulation of GTPase Activity of G Proteins by Fluid Shear Stress and Phospholipid Composition. *Proc. Natl. Acad. Sci. U.S.A.* **1998**, *95*, 2515−2519.

(4) Yamashita, K.; Miyazaki, M.; Yamaguchi, Y.; Nakamura, H.; Maeda, H. Thermodynamic Properties of Duplex DNA in Microchannel Laminar Flow. *ChemPhysChem* **2007**, *8*, 1307−1310.

(5) Schneider, S. W.; Nuschele, S.; Wixforth, A.; Gorzelanny, C.; Alexander-Katz, A.; Netz, R. R.; Schneider, M. F. Shear-Induced Unfolding Triggers Adhesion of von Willebrand Facror Fibers. *Proc. Natl. Acad. Sci. U.S.A.* **2007**, *104*, 7899−7903.

(6) Bekard, I. B.; Asimakis, P.; Teoh, C. L.; Ryan, T.; Howlett, G. J.; Bertolini, J.; Dunstan, D. E. Bovine Serum Albumin Unfolds in Couette Flow. *Soft Matter* **2012**, *8*, 385−389.

(7) Jaspe, J.; Hagen, S. J. Do Protein Molecules Unfold in a Simple Shear Flow? *Biophys. J.* **2006**, *91*, 3415−3424.

(8) Korin, N.; Kanapathipillai, M.; Matthews, B. D.; Crescente, M.; Brill, A.; Mammoto, T.; Ghosh, K.; Jurek, S.; Bencherif, S. A.; Bhatta, D.; Coskun, A. U.; Feldman, C. L.; Wagner, D. D.; Ingber, D. E. Shear-Activated Nanotherapeutics for Drug Targeting to Obstructed Blood Vessels. *Science* **2012**, *337*, 738−742.

(9) Hallow, D. M.; Seeger, R. A.; Kamaev, P. P.; Prado, G. R.; LaPlaca, M. C.; Prausnitz, M. R. Shear-Induced Intracellular Loading of Cells with Molecules by Controlled Microfluidics. *Biotechnol. Bioeng.* **2008**, *99*, 846−854.

(10) Holme, M. N.; Fedotenko, I. A.; Abegg, D.; Althaus, J.; Babel, L.; Favarger, F.; Reiter, R.; Tanasescu, R.; Zaffalon, P.- L.; Ziegler, A.; Müller, B.; Saxer, T.; Zumbuehl, A. Shear-Stress Sensitive Lenticular Vesicles for Targeted Drug Delivery. *Nat. Nanotechnol.* **2012**, *7*, 536−543.

(11) Fedotenko, I. A.; Zaffalon, P.- L.; Favarger, F.; Zumbuehl, A. The Synthesis of 1,3-Diamidophospholipids. *Tetrahedron Lett.* **2010**, *51*, 5382−5384.

(12) Seong, G. H.; Crooks, R. M. Efficient Mixing and Reactions within Microfluidic Channels Using Microbead-Supported Catalysts. *J. Am. Chem. Soc.* **2002**, *124*, 13360−13361.

(13) He, J.; Wang, L.; Wei, Z.; Yang, Y.; Wang, C.; Han, X.; Nie, Z. Vesicular Self-Assembly of Colloidal Amphiphiles in Microfluidics. *ACS Appl. Mater. Interfaces* **2013**, *5*, 9746−9751.

(14) Yamada, M.; Kasim, V.; Nakashima, M.; Edahiro, J.; Seki, M. Continuous Cell Partitioning Using an Aqueous Two-Phase Flow System in Microfluidic Devices. *Biotechnol. Bioeng.* **2004**, *88*, 489−494.

(15) Sun, B. J.; Shum, H. C.; Holtze, C.; Weitz, D. A. Microfluidic Melt Emulsification for Encapsulation and Release of Actives. *ACS Appl. Mater. Interfaces* **2010**, *2*, 3411−3416.

(16) Tanaka, Y.; Slyadnev, M. N.; Sato, K.; Tokeshi, M.; Kim, H.- B.; Kitamori, T. Acceleration of an Enzymatic Reaction in a Microchip. *Anal. Sci.* **2001**, *17*, 809−810.

(17) Kanno, K.; Maeda, H.; Izumo, S.; Ikuno, M.; Takeshita, K.; Tashiro, A.; Fujii, M. Rapid Enzymatic Transglycosylation and Oligosaccharide Synthesis in a Microchip Reactor. *Lab Chip* **2002**, *2*, 15−18.

(18) Wang, C.; Ye, D. -K.; Wang, Y.-Y.; Lu, T.; Xia, X.-H. Insights into the "Free State" Enzyme Reaction Kinetics in Nanoconfinement. *Lab Chip* **2013**, *13*, 1546−1553.

(19) Charm, S. E.; Wong, B. L. Enzyme Inactivation with Shearing. *Biotechnol. Bioeng.* **1970**, *12*, 1103−1109.

(20) Bekard, I. B.; Asimakis, P.; Bertolini, J.; Dunstan, D. E. The Effects of Shear Flow on Protein Structure and Function. *Biopolymers* **2011**, *95*, 733−745.

(21) van der Veen, M. E.; van Iersel, D. G.; van der Goot, A. J.; Boom, R. M. Shear-Induced Inactivation of α-Amylase in a Plain Shear Field. *Biotechnol. Prog.* **2004**, *20*, 1140−1145.

(22) Ashton, L.; Dusting, J.; Imomoh, E.; Balabani, S.; Blanch, E. W. Shear-Induced Unfolding of Lysozyme Monitored In Situ. *Biophys. J.* **2009**, *96*, 4231−4236.

(23) Hartl, F. U. Molecular Chaperones in Cellular Protein Folding. *Nature* **1996**, *381*, 571−580.

(24) Mangione, P. P.; Esposito, G.; Relini, A.; Raimondi, S.; Porcari, R.; Giorgetti, S.; Corazza, A.; Fogolari, F.; Penco, A.; Goto, Y.; Lee, Y.-H.; Yagi, H.; Cecconi, C.; Naqvi, M. M.; Gillmore, J. D.; Hawkins, P. N.; Chiti, F.; Rolandi, R.; Taylor, G. W.; Pepys, M. B.; Stoppini, M.; Bellotti, V. Structure, Folding Dynamics, and Amyloidogenesis of D76N β_2-Microglobulin. Roles of Shear Flow, Hydrophobic Surfaces, and α-Crystallin. *J. Biol. Chem.* **2013**, *288*, 30917−30930.

(25) Takahashi, H.; Sawada, S.; Akiyoshi, K. Amphiphilic Polysaccharide Nanoballs: A New Building Block for Nanogel Biomedical Engineering and Artificial Chaperones. *ACS Nano* **2011**, *5*, 337−345.

(26) Kameta, N.; Masuda, M.; Shimizu, T. Soft Nanotube Hydrogels Functioning as Artificial Chaperones. *ACS Nano* **2012**, *6*, 5249−5258.

(27) Osaki, M.; Takashima, Y.; Yamaguchi, H.; Harada, A. An Artificial Molecular Chaperone: Poly-Pseudo-Rotaxane with an Extensible Axle. *J. Am. Chem. Soc.* **2007**, *129*, 14452−14457.

(28) Kuboi, R.; Yoshimoto, M.; Walde, P.; Luisi, P. L. Refolding of Carbonic Anhydrase Assisted by 1-Palmitoyl-2-Oleoyl-sn-Glycero-3-Phosphocholine Liposomes. *Biotechnol. Prog.* **1997**, *13*, 828−836.
(29) Yoshimoto, M.; Kuboi, R. Oxidative Refolding of Denatured/Reduced Lysozyme Utilizing the Chaperone-Like Function of Liposomes and Immobilized Liposome Chromatography. *Biotechnol. Prog.* **1999**, *15*, 480−487.
(30) Yoshimoto, M.; Tamura, R.; Natsume, T. Liposome Clusters with Shear Stress-Induced Membrane Permeability. *Chem. Phys. Lipids* **2013**, *174*, 8−16.
(31) Natsume, T.; Yoshimoto, M. A Method to Estimate the Average Shear Rate in a Bubble Column Using Liposomes. *Ind. Eng. Chem. Res.* **2013**, *52*, 18498−18502.
(32) Yoshimoto, M.; Miyazaki, Y.; Sato, M.; Fukunaga, K.; Kuboi, R.; Nakao, K. Mechanism for High Stability of Liposomal Glucose Oxidase to Inhibitor Hydrogen Peroxide Produced in Prolonged Glucose Oxidation. *Bioconjugate Chem.* **2004**, *15*, 1055−1061.
(33) Yoshimoto, M.; Wang, S.; Fukunaga, K.; Fournier, D.; Walde, P.; Kuboi, R.; Nakao, K. Novel Immobilized Liposomal Glucose Oxidase System Using the Channel Protein OmpF and Catalase. *Biotechnol. Bioeng.* **2005**, *90*, 231−238.
(34) Kim, J.; Khan, M.; Park, S.- Y. Glucose Sensor Using Liquid-Crystal Droplets Made by Microfluidics. *ACS Appl. Mater. Interfaces* **2013**, *5*, 13135−13139.
(35) Nakao, K.; Harada, T.; Furumoto, K.; Kiefner, A.; Popovic, M. Mass Transfer Properties of Bubble Columns Suspending Immobilized Glucose Oxidase Gel Beads for Gluconic Acid Production. *Can. J. Chem. Eng.* **1999**, *77*, 816−825.
(36) Swoboda, B. E. P.; Massey, V. Purification and Properties of the Glucose Oxidase from Aspergillus niger. *J. Biol. Chem.* **1965**, *240*, 2209−2215.
(37) MacDonald, R. C.; MacDonald, R. I.; Menco, B. P. M.; Takeshita, K.; Subbarao, N. K.; Hu, L. R. Small-Volume Extrusion Apparatus for Preparation of Large, Unilamellar Vesicles. *Biochim. Biophys. Acta* **1991**, *1061*, 297−303.
(38) Takayama, M.; Ito, S.; Nagasaki, T.; Tanimizu, I. A New Enzymatic Method for Determination of Serum Choline-Containing Phospholipids. *Clin. Chim. Acta* **1977**, *79*, 93−98.
(39) Hill, K. J.; Kaszuba, M.; Creeth, J. E.; Jones, M. N. Reactive Liposomes Encapsulating a Glucose Oxidase-Peroxidase System with Antibacterial Activity. *Biochim. Biophys. Acta* **1997**, *1326*, 37−46.
(40) Yoshimoto, M.; Wang, S.; Fukunaga, K.; Walde, P.; Kuboi, R.; Nakao, K. Preparation and Characterization of Reactive and Stable Glucose Oxidase-Containing Liposomes Modulated with Detergent. *Biotechnol. Bioeng.* **2003**, *81*, 695−704.
(41) Yoshimoto, M.; Sakamoto, H.; Yoshimoto, N.; Kuboi, R.; Nakao, K. Stabilization of Quaternary Structure and Activity of Bovine Liver Catalase through Encapsulation in Liposomes. *Enzyme Microb. Technol.* **2007**, *41*, 849−858.
(42) Huggett, A. S. T.; Nixon, D. A. Use of Glucose Oxidase, Peroxidase, and o-Dianisidine in Determination of Blood and Urinary Glucose. *Lancet* **1957**, *273*, 368−370.
(43) Bird, R. B.; Stewart, W. E.; Lightfoot, E. N. *Transport Phenomena*, 2nd ed; John Wiley & Sons: New York, 2007; pp 48−53.
(44) Yoshimoto, M.; Miyazaki, Y.; Umemoto, A.; Walde, P.; Kuboi, R.; Nakao, K. Phosphatidylcholine Vesicle-Mediated Decomposition of Hydrogen Peroxide. *Langmuir* **2007**, *23*, 9416−9422.
(45) Yoshimoto, M.; Monden, M.; Jiang, Z.; Nakao, K. Permeabilization of Phospholipid Bilayer Membranes Induced by Gas-Liquid Flow in an Airlift Bubble Column. *Biotechnol. Prog.* **2007**, *23*, 1321−1326.
(46) Kuroiwa, T.; Fujita, R.; Kobayashi, I.; Uemura, K.; Nakajima, M.; Sato, S.; Walde, P.; Ichikawa, S. Efficient Preparation of Giant Vesicles as Biomimetic Compartment Systems with High Entrapment Yields for Biomacromolecules. *Chem. Biodivers.* **2012**, *9*, 2453−2472.
(47) Yoshimoto, M.; Wang, S.; Fukunaga, K.; Treyer, M.; Walde, P.; Kuboi, R.; Nakao, K. Enhancement of Apparent Substrate Selectivity of Proteinase K Encapsulated in Liposomes through a Cholate-Induced Alteration of the Bilayer Permeability. *Biotechnol. Bioeng.* **2004**, *85*, 222−233.
(48) Sabín, J.; Prieto, G.; Sarmiento, F. Stable Clusters in Liposomic Systems. *Soft Matter* **2012**, *8*, 3212−3222.
(49) Sabín, J.; Prieto, G.; Ruso, J. M.; Sarmiento, F. Fractal Aggregates Induced by Liposome-Liposome Interaction in the Presence of Ca^{2+}. *Eur. Phys. J. E* **2007**, *24*, 201−210.
(50) Donato, L. D.; Cataldo, M.; Stano, P.; Massa, R.; Ramundo-Orland, A. Permeability Changes of Cationic Liposomes Loaded with Carbonic Anhydrase Induced by Millimeter Waves Radiation. *Rad. Res* **2012**, *178*, 437−446.
(51) Miyazaki, M.; Nakamura, H.; Maeda, H. Improved Yield of Enzyme Reaction in Microchannel Reactor. *Chem. Lett.* **2001**, *30*, 442−443.
(52) Yamashita, K.; Miyazaki, M.; Nakamura, H.; Maeda, H. Nonimmobilized Enzyme Kinetics That Rely on Laminar Flow. *J. Phys. Chem. A* **2009**, *113*, 165−169.